SIAM J. SCI. COMPUT.
Vol. 21, No. 4, pp. 1222–1243

A STABLE NUMERICAL METHOD FOR INVERTING SHAPE FROM MOMENTS*

GENE H. GOLUB†, PEYMAN MILANFAR‡, AND JAMES VARAH§

Abstract. We derive a stable technique, based upon matrix pencils, for the reconstruction of (or approximation by) polygonal shapes from moments. We point out that this problem can be considered the dual of $2-D$ numerical quadrature over polygonal domains. An analysis of the sensitivity of the problem is presented along with some numerical examples illustrating the relevant points. Finally, an application to the problem of gravimetry is explored where the shape of a gravitationally anomalous region is to be recovered from measurements of its exterior gravitational field.

Key words. shape, inversion, moments, matrix pencils, polygon, ill-conditioned, quadrature, gravimetry

AMS subject classifications. 65F15, 65D32, 44A60, 65F35, 65E05, 94A12, 86A20

PII. S1064827597328315

1. Introduction.

This paper is concerned with solving a variety of inverse problems, using tools from the method of moments. The problem of reconstructing a function and/or its domain given its moments is ubiquitous in both pure and applied mathematics. Numerous applications from diverse areas such as probability and statistics [8], signal processing [33], computed tomography [26, 27], and inverse potential theory [4, 35] (magnetic and gravitational anomaly detection) can be cited, to name just a few. In statistical applications, time-series data may be used to estimate the moments of the underlying density, from which an estimate of this probability density may be sought. In computed tomography, the X-rays of an object can be used to estimate the moments of the underlying mass distribution, and from these the shape of the object being imaged may be estimated [26, 27]. Also, in geophysical applications, the measurements of the exterior gravitational field of a region can be readily converted into moment information, and from these, the shape of the region may be determined. We will discuss this last application later in this paper.

In all its many guises, the moment problem is universally recognized as a notoriously difficult inverse problem which often leads to the solution of very ill-posed systems of equations that usually do not have a unique solution. The series of problems treated in the present paper related to the reconstruction (or polygonal approximation) of the shape of a plane region of constant density from its (harmonic) moments are in most respects no different; they too suffer from the numerical instabilities and the solutions are not always unique. However, several aspects of what we shall henceforth call the shape-from-moments problem render this a rather interesting topic. The first is that, contrary to most cases, this particular manifestation of the moment

*Received by the editors October 6, 1997; accepted for publication (in revised form) June 30, 1998; published electronically December 9, 1999.
http://www.siam.org/journals/sisc/21-4/32831.html

†Department of Computer Science, Stanford University, Stanford, CA 94305 (golub @ sccm.stanford.edu). The work of this author was supported in part by NSF grant CCR-9505393.

‡SRI International, 333 Ravenswood Ave. (M/S 404-69), Menlo Park, CA 94025 (milanfar @unix.sri.com).

§Department of Computer Science, University of British Columbia Centre for Integrated Computer Systems Research, 2053-2324 Main Mall, Vancouver, BC V6T 1W5, Canada (varah@cs.ubc.edu).

problem allows a complete, closed-form solution. More remarkable still is the fact that the solutions are based on techniques of numerical linear algebra, such as generalized eigenvalue problems, which not only yield stable and fast algorithms but also expose a seemingly deep connection between the shape-from-moments problem and the theory of numerical quadrature over planar regions. In fact, this connection is so fundamental that one may consider the two problems as duals. At the same time, the techniques for solving the shape reconstruction problem are intimately related to so-called array processing techniques [23, 25].

Another interesting, and useful, feature of the shape-from-moments problem is that despite its relative simplicity, it is applicable to a wide variety of inverse problems of interest. Consider the following diverse set of examples:

- A region of the plane can be regarded as the domain of a (uniform) probability density function. In this case, the problem is that of reconstructing, or approximating, the domain by a polygon from measurements of its moments [8].
- Tomographic (line integral) measurements of a body of constant density can be converted into moments from which an approximation to its boundary can be extracted [27].
- Measurements of exterior gravitational field induced by a body of uniform mass can be turned into moment measurement, from which the shape of the region may be reconstructed [35]. (We discuss this application in section 6.)
- Measurements of exterior magnetic field induced by a body of uniform magnetization can yield measurement of the moments of the region from which the shape of the region may be determined [35].
- Measurements of thermal radiation made outside a uniformly hot region can yield moment information, which can subsequently be inverted to give the shape of the region [35].

In fact, inverse problems for uniform density regions related to general elliptical equations can all be cast as moment problems which fall within the scope of application of the results of this paper. To maintain focus, however, we first approach the shape-from-moments problem directly and without reference to a particular application.

In section 2 we provide the mathematical and historical background behind the results of this paper, present some basic definitions and review the work in a previous paper [27]. Section 3 contains our results for shape reconstruction from moments using matrix pencil techniques. In section 4 we describe how to improve the conditioning of the problem by appropriate scaling of the matrix pencils and give an explicit description of the algorithm. In section 5 we discuss how one might choose the best number of vertices to fit to a given sequence of (possibly noise-corrupted) moments. In section 6 we discuss an application of the results to the inverse gravimetric problem. Finally, in section 7 we provide some numerical examples to support our results; and we state our conclusions and summarize our results in section 8.

2. Background. During a luncheon conversation over 45 years ago, Motzkin and Schoenberg discovered a beautiful quadrature formula over triangular regions of the complex plane [32]. Namely, given a function $f(z)$, analytic in the closure of a triangle T, they showed that the integral of the second derivative $f''(z)$ with respect to the area measure $dx\,dy$ is proportional to the second divided difference of f with respect to the vertices z_1, z_2, z_3, of the triangle, with the proportionality constant being twice the area of T. Later, Davis [6, 7] generalized this result to polygonal regions.

THEOREM 2.1 (see Davis [6, 7]). *Let $z_1, z_2, \ldots, z_n$ designate the vertices of a polygon P in the complex plane. Then we can find constants $a_1, \ldots, a_n$ depending upon $z_1, z_2, \ldots, z_n$, but independent of f, such that for all f analytic in the closure of P,*

$$\int\int_P f''(z)\, dx\, dy = \sum_{j=1}^{n} a_j f(z_j). \tag{2.1}$$

When the left-hand side is being sought, the above formula is, of course, a quadrature formula. However, let us assume for a moment that the region P is unknown but that its moments with respect to some basis such as $\{z^k\}$ are given. Replacing the function $f(z)$ with the elements of this basis in (2.1) results in an expression proportional to the moments on the left-hand side, while the unknown vertices z_j appear on the right-hand side. The shape-from-moments problem then is concerned with solving for the unknown vertices and amplitudes a_j from knowledge of these moments.

Returning to Theorem 2.1, if we assume that the vertices z_j of P are arranged, say, in the counterclockwise direction in the order of increasing index, and extending the indexing of the z_j cyclically, so that $z_0 = z_n$, $z_1 = z_{n+1}$, the coefficients a_j can be written as (see [7])

$$a_j = \frac{i}{2}\left(\frac{\overline{z}_{j-1} - \overline{z}_j}{z_{j-1} - z_j} - \frac{\overline{z}_j - \overline{z}_{j+1}}{z_j - z_{j+1}}\right). \tag{2.2}$$

The expression for a_j has a naturally intuitive interpretation. If ϕ_j denotes the angle of the side $\langle z_j z_{j+1}\rangle$ with the positive real axis, then

$$\alpha_j = \frac{\overline{z}_j - \overline{z}_{j+1}}{z_j - z_{j+1}} = e^{-2i\phi_j}, \tag{2.3}$$

where $i = \sqrt{-1}$. In fact, α_j is in essence the complex analogue of *slope* for the line $\langle z_j z_{j+1}\rangle$. Hence, the coefficients $a_j = (e^{-2i\phi_{j-1}} - e^{-2i\phi_j})\frac{i}{2}$ can be interpreted as the difference in slope of the two sides meeting at the vertex z_j. Therefore, the a_j are nonzero if, and only if, the polygon is nondegenerate. Furthermore, these coefficients can be written even more succinctly as

$$a_j = \sin(\phi_{j-1} - \phi_j) e^{-i(\phi_{j-1} + \phi_j)}, \tag{2.4}$$

which shows that for a nondegenerate polygon, $0 < |a_j| \leq 1$. When $|a_j|$ is unity, we have a right angle at vertex z_j, whereas when $|a_j|$ is near zero, the polygon is nearly degenerate at that vertex.

Moments and reconstruction. Defining the *harmonic* moments of an n-sided polygonal region P by

$$c_k = \int\int_P z^k\, dx\, dy, \tag{2.5}$$

we can compute these directly by invoking Theorem 2.1. Namely, by replacing $f(z) = z^k$, we get

$$\int\int_P (z^k)''\, dx\, dy = k(k-1)\int\int_P z^{k-2}\, dx\, dy = k(k-1)c_{k-2} = \sum_{j=1}^{n} a_j z_j^k. \tag{2.6}$$

The *complex* moments τ_k are then defined as

$$\tau_k \equiv k(k-1)c_{k-2} = \sum_{j=1}^{n} a_j z_j^k, \tag{2.7}$$

where, by definition, $\tau_0 = \tau_1 = 0$. In [27] we showed that given $c_0, c_1, \ldots, c_{2n-3}$, or, equivalently, $\tau_0, \tau_1, \ldots, \tau_{2n-1}$, the vertices of the n-gon can be uniquely recovered. In [27] this was accomplished using Prony's method [19, p. 456] whereby due to (2.7) we can write

$$\begin{bmatrix} \tau_0 & \tau_1 & \cdots & \tau_{n-1} \\ \tau_1 & \tau_2 & \cdots & \tau_n \\ \vdots & \vdots & \ddots & \vdots \\ \tau_{n-1} & \tau_n & \cdots & \tau_{2n-2} \end{bmatrix} p^{(n)} = - \begin{bmatrix} \tau_n \\ \tau_{n+1} \\ \vdots \\ \tau_{2n-1} \end{bmatrix}, \tag{2.8}$$

$$H_0 p^{(n)} = -h_n, \tag{2.9}$$

where $p^{(n)} = [p_n, p_{n-1}, \ldots, p_1]^T$ contains the coefficients of the polynomial $P(z) = \prod_{j=1}^{n}(z - z_j) = z^n + \sum_{j=1}^{n} p_j z^{n-j}$, whose roots are the vertices we seek. The sensitivity of this technique (and its least squares variants studied in [27]) is affected by two factors. First, to solve for the coefficient vector $p^{(n)}$, the ill-conditioned linear system of equations (2.9) must be solved. Next, the sensitivity of the roots of the polynomial $P(z)$ to perturbations in its coefficients cause further inaccuracies in the resulting estimates of the vertices.

Hankel matrices in general, and the Hankel matrix H_0, in particular, can be severely ill-conditioned [36]. This can be seen by noting that the "signal model" in (2.7) implies a decomposition [21, 25, 27] of H_0 as

$$H_0 = V_n \mathrm{diag}(\mathbf{a}_n) V_n^T, \tag{2.10}$$

where V_n is the *Vandermonde* matrix of the vertices $\{z_j\}$

$$V_n = \begin{bmatrix} 1 & 1 & \cdots & 1 \\ z_1 & z_2 & \cdots & z_n \\ \vdots & \vdots & \ddots & \vdots \\ z_1^{n-1} & z_2^{n-1} & \cdots & z_n^{n-1} \end{bmatrix} \tag{2.11}$$

and $\mathbf{a}_n = [a_1,\ a_2, \ldots, a_n]^T$.

3. Pencil-based reconstruction. In the basis $\{z^k\}$, the moment expression (2.7) can be used to construct two Hankel matrices H_0 (as in (2.9)) and H_1, which has the same form as H_0 but starts with τ_1 instead of τ_0 and ends with τ_{2n-1}. As we indicated earlier, these matrices have the following useful factorizations:

$$H_0 = V D V^T, \tag{3.1}$$

$$H_1 = V D Z V^T, \tag{3.2}$$

where for simplicity $V = V_n$, $Z = \mathrm{diag}(z_1, \ldots, z_n)$, and $D = \mathrm{diag}(\mathbf{a}_n)$. Therefore, H_0 and H_1 are simultaneously diagonalized by V^{-1}:

$$V^{-1} H_0 V^{-T} = D, \tag{3.3}$$

$$V^{-1} H_1 V^{-T} = DZ, \tag{3.4}$$

and hence the generalized eigenvalue problem

$$H_1\mu = zH_0\mu \tag{3.5}$$

has the solutions $\{z_j\}$ which are the polygon vertices we seek.

The pencil problem can be more generally formulated over a different polynomial basis. Analogous to the theory of *modified moments* [11, 14], this can be accomplished as follows. Consider a basis $\{p_k(z)\}$ of polynomials constructed from a linear combination of the elements of $\{z^k\}$. For each vertex z_j of the underlying polygon we can write

$$\mathbf{p}(z_j) = \Phi\mathbf{w}(z_j), \tag{3.6}$$

where Φ is a lower-triangular matrix with $\det(\Phi) \neq 0$, and

$$\mathbf{p}(z_j) = \begin{bmatrix} p_0(z_j) \\ p_1(z_j) \\ \vdots \\ p_{n-1}(z_j) \end{bmatrix}, \quad \mathbf{w}(z_j) = \begin{bmatrix} 1 \\ z_j \\ \vdots \\ z_j^{n-1} \end{bmatrix}. \tag{3.7}$$

We refer to the moments in this new basis as the *transformed moments*. The Hankel matrices corresponding to these transformed moments are

$$\mathbf{H}_0 = \Phi H_0 \Phi^T, \tag{3.8}$$

$$\mathbf{H}_1 = \Phi H_1 \Phi^T. \tag{3.9}$$

These Hankel matrices are simultaneously diagonalized by $(V\Phi)^{-1}$ so that

$$(V\Phi)^{-1}\mathbf{H}_0(V\Phi)^{-T} = D, \tag{3.10}$$

$$(V\Phi)^{-1}\mathbf{H}_1(V\Phi)^{-T} = DZ. \tag{3.11}$$

Therefore, the generalized eigenvalue problem

$$\mathbf{H}_1\mathbf{u} = z\mathbf{H}_0\mathbf{u} \tag{3.12}$$

has the *same* solutions $\{z_j\}$ as the pencil in (3.5). However, the last identity is a more general form of the pencil in (3.5). In particular, (3.12) implies (3.5) when Φ is the identity matrix. It is interesting to compare (3.12) with the matrix pencil solution of the signal decomposition problem derived by Luk and Vandevoorde [25, p. 344]. They introduce two unspecified nonsingular transformations F and G which in our context of transformed moments are simply Φ and Φ^T. As the authors correctly point out, the choice of F and G will affect the efficiency and accuracy of the overall problem. In section 4 of this paper, we outline a procedure for choosing *diagonal* scaling matrices Φ that will improve the condition of the matrix pencil solution to the problem of reconstructing vertices from moments.

It is important to point out that while the matrix pencil formulation has been extensively studied in the array processing literature [21, 23, 31], our treatment is more general in that (1) it does not make the assumption that the roots (vertices) reside on the unit circle, and (2) our approach is formulated over a general polynomial basis.

In any case, both forms (3.5) and (3.12) are interesting from the point of view of numerical computation for generalized eigenvalue problems. (See [15, 28], for example.) Since H_0 is nonsingular, (3.5) is a regular (not singular) problem. However, as we shall see in the numerical examples of section 7, both H_0 and H_1 can be very ill-conditioned, and in fact (3.5) can have "ill-disposed" eigenvalues, where the corresponding eigenvectors are very nearly mapped into zero by both H_0 and H_1. This occurs whenever some $|a_j|$ is small, as can be seen from the factorization (3.1). As we mentioned earlier, $|a_j|$ will be small whenever the interior angle at z_j is either close to zero or 180°.

Various algorithms can be used for the solution of (3.5) or (3.12). However, since H_0 is ill-conditioned, one should not use a computational technique that involves inverting H_0. In fact, since H_0 and H_1 are complex symmetric matrices, the solution of the generalized eigenvalue problem can be obtained most stably by the QZ algorithm[1] [15]. One can improve on the usual QZ algorithm here, because of the special form of H_0 and H_1, as follows: normally, the first stage of QZ involves unitary transformations on H_0 and H_1, on both the left and right, to take H_0 into triangular form and H_1 into upper Hessenberg form. This computation requires about $8n^3$ flops [15, Algorithm 7.7.1, p. 38]. However, because of the replication of columns of H_0 within H_1, one can instead form the QR factorization of H_0 augmented by the last column of H_1. Then the first n columns of the $n \times (n+1)$ matrix R form the (square) triangular matrix $R' = Q'H_0$, and the last n columns form the upper Hessenberg matrix $H' = Q'H_1$. This QR step requires only about $(4/3)n^3$ flops [15, p. 225], roughly one-sixth that of the normal QZ step. Finally, the second (iterative) stage of QZ can be applied to the pair (H',R').

It is worth noting here that in the above argument the essential requirement is the replication of the columns, not the Hankel structure of the matrices. Thus, the idea is more generally applicable (to the *generalized* Hankel matrix in (3.12), for example), and we intend to expand on this issue in a subsequent paper.

3.1. Estimation of a_j. Once the vertices z_j have been determined, there exist several techniques for computing the coefficients a_j. In general, since the ordering of the vertices is not known a priori, we cannot use (2.2). Perhaps the simplest technique is to use (2.7) for $k = 0, \ldots, n-1$ and solve

$$V\mathbf{a}_n = \mathcal{T}_n, \tag{3.13}$$

where $\mathcal{T}_n = [\tau_0, \tau_1, \ldots, \tau_{n-1}]^T$. As one referee suggested, a fast Vandermonde solver can be used for (3.13). These can be more accurate for some data vectors $\mathcal{T}_n$ with particular orderings of the z_j's. (See Higham [18, p. 434].) This topic requires further investigation.

One could also use all the available moments and solve a similar linear system via least squares. In either case, it is useful to note that the first two rows of (3.13) corresponding to $\tau_0 = \tau_1 = 0$ should be treated as linear *constraints* rather than data. Doing this yields a smaller linear problem (by two rows), with a pair of linear constraints. These constraints act, in essence, to regularize the problem and hence we can obtain more accurate results than those reported in [27].

Alternatively, one could directly obtain the coefficients a_j by forming the Vandermonde matrix $\widehat{V}$ from the estimated vertices and computing the diagonals of

[1] It is interesting to note, as also pointed out in [25], that the companion matrix for the polynomial $P(z)$ can be written as $H_0^{-1}H_1$. As this involves the inverse of H_0, this indicates why the Prony method is sensitive to small perturbations.

$\widehat{V}^{-1}H_0\widehat{V}^{-T}$. Finally, one can use the computed eigenvectors μ_j from the QZ process which are *scaled* columns of V^{-T}. That is, if M has μ_j as columns, then

$$M = V^{-T}S, \tag{3.14}$$

where S is a diagonal scaling matrix which is yet to be determined. To determine S, note that $T = M^{-1} = S^{-1}V^T$ and that we want the first column of V^T to contain all ones (since V has Vandermonde structure). That is, the diagonal elements of S must be given by the solution of

$$[S]_{j,j}T_{j,1} = 1, \tag{3.15}$$

where $T_{j,1}$'s denote the elements of the first column of $T = M^{-1}$. Because we have the scaling factors, the expression for the coefficients a_j becomes

$$a_j = \left(\mu_j^T H_0 \mu_j\right)(T_{j,1})^2. \tag{3.16}$$

Our experiments show that both techniques (based on (3.13) and (3.16)) appear to give roughly the same accuracy.

3.2. Reconstruction of the interior of the polygon. As discussed in [27] and [35], unless the underlying polygon is assumed to be convex, the estimation of the vertices does not necessarily yield a unique reconstruction of the interior of the polygon. In fact, in some (rather rare and complex) circumstances, it is impossible to find the interior of the polygon uniquely, even if both the vertices z_j and the coefficients a_j are given.

For the majority of cases where a unique solution does exist, given z_j and the corresponding a_j, a mechanism must be devised to actually "connect the dots" and obtain the interior of the polygon. One such mechanism may proceed as follows. Recall the expression

$$a_j = \sin(\phi_{j-1} - \phi_j)e^{-i(\phi_{j-1}+\phi_j)}, \tag{3.17}$$

where ϕ_j denotes the angle of the side j (namely, $\langle z_j z_{j+1}\rangle$) with the positive real axis. Knowledge of a_j implies that we can write

$$\phi_{j-1} - \phi_j = \arcsin(|a_j|) + 2l_1\pi, \tag{3.18}$$

$$\phi_{j-1} + \phi_j = \arctan\left(\frac{\mathrm{Im}\{a_j\}}{\mathrm{Re}\{a_j\}}\right) + l_2\pi \tag{3.19}$$

for some integers $\{l_1, l_2\} = \{0, \pm 1, \ldots\}$. Solving the above system of equations for each j, and observing the condition that the resulting polygon is simply connected and closed, we can compute each angle ϕ_j to within an integer multiple of $\pi/2$. Hence, given n vertices, in general there exists a total of at most 2^{n-1} possible configurations (ways of laying down the sides). This number of combinations is exponential in n and a more efficient technique is needed to uniquely determine the interior of the (simply connected) polygon. We view this as an interesting problem in computational geometry and one which is outside the scope of the present paper.

3.3. Analysis of sensitivity. The sensitivity of the vertices with respect to perturbations in the moments can be computed from the eigenvalue sensitivity of the matrix pencil problem $H_1\mu = zH_0\mu$. Consider a simple eigenvalue (z) of this pencil and write an ϵ-perturbation of the system

$$(H_1 + \epsilon F)(\mu + \epsilon\mu^{(1)} + \cdots) = (z + \epsilon z^{(1)} + \cdots)(H_0 + \epsilon G)(\mu + \epsilon\mu^{(1)} + \cdots). \tag{3.20}$$

Retaining only the first-order terms gives

$$(H_1 - zH_0)\mu^{(1)} = (z^{(1)}H_0 + zG - F)\mu, \tag{3.21}$$

and we wish to find an expression for $z^{(1)}$ which measures the first-order sensitivity. We next multiply (3.21) on the left by the (left) eigenvector μ (which in this case coincides with the right eigenvector, as H_0 and H_1 are complex symmetric). This action annihilates the left-hand side of (3.21), and after simplifying we get

$$z^{(1)} = \frac{\mu^T(F - zG)\mu}{\mu^T H_0 \mu}. \tag{3.22}$$

If we now assume that μ is normalized so that $\|\mu\| = 1$ and $\|F\|_2 = \|H_1\|_2$, $\|G\|_2 = \|H_0\|_2$, we have

$$|z_j^{(1)}| \leq \frac{\|H_1\|_2 + |z|\|H_0\|_2}{|\mu_j^T H_0 \mu_j|}. \tag{3.23}$$

The important term in the above is the denominator; when this is small, we have what we described earlier as an "ill-disposed" eigenvalue. Recalling the expression (3.16) for a_j, we see that the ill-disposed vertex occurs when $|a_j|$ is small, or when the Vandermonde matrix is ill-conditioned. We note here that we could obtain even tighter bounds for the perturbation coefficients $z_j^{(1)}$ by restricting the perturbations F and G allowed to those having Hankel structure. However, the resulting expressions are much more complicated, and in practice we have found (3.23) to reflect the actual sensitivities quite well. For more detailed investigation of these sensitivities, the reader is referred to [10, 17].

In summary, the general problem of vertex reconstruction from moments can be seen to suffer from three inherent sources of sensitivity. The first, addressed in the next section, is related to the scaling of the problem (i.e., vertices closer to the unit circle are less sensitive). The second has to do with the size of $|a_j|$ which is directly related to the angle at the corresponding vertex (vertices at angles near zero or 180◦ are most sensitive). Finally, the relative position of the vertices (e.g., close together without being collinear, or collinear without being on the same edge) can adversely affect the condition of the Vandermonde matrix V and hence the solution in general. It is worth noting that significant roundoff error can certainly cause the reconstruction to fail. In our experience, in this respect, convex polygons are easier to reconstruct and less prone to effects of roundoff errors and noise, unless the shape is rather elongated and eccentric. This will cause the condition of the problem to be rather large and therefore amplify the effect of roundoff error. The sensitivity analysis presented above confirms these observations.

4. Improving condition via transformed moments. As can be seen from (2.10), the condition number of H_0 is related quadratically to the condition of V_n and directly to the condition of $\mathrm{diag}(\mathbf{a}_n)$. For its part, the condition number of V_n grows exponentially large (see [12, 36] and the following subsection) with the number of vertices n as ρ^{n-1} where $\rho = \max_j |z_j|$ (> 1) or as $(1/\rho)^{n-1}$ when $\rho < 1$. On the other hand, the condition of $\mathrm{diag}(\mathbf{a}_n)$ is related to the size of the smallest coefficient $|a_j|$. Therefore, the geometry of the underlying polygon has a great effect on the sensitivity of the solution. But this source of instability is inherent and, strictly speaking, cannot be remedied. However, a treatable factor that plays an important

part in making the reconstruction problem ill-conditioned is scaling. We will show, in this section, that much can be done in the way of improving the scaling and therefore the condition of the problem.

The moments c_k are measured with respect to the basis $\{z^k\}$. This family is orthogonal [5] over any disk $D(0,r)$ centered at the origin with radius r; namely,

$$\iint_{D(0,r)} z^k \bar{z}^l \, dx \, dy = \begin{cases} 0, & k \neq l, \\ \pi \, r^{2(k+1)}/(k+1), & k = l. \end{cases} \tag{4.1}$$

However, as the size of the underlying polygon (as measured by $\rho = \max_j |z_j|$) may be significantly different from r, this may cause the Hankel matrix H_0 to be badly scaled; that is, the higher-order moments can grow (or diminish) quite quickly in size. In fact, (2.7) shows that $|c_k|$ grows as ρ^{k+2} and $|\tau_k|$ grows as ρ^k.

To alleviate the difficulties related to scaling, we redefine these moments in a scaled (and shifted) basis. First, we note that if the polygon's center of mass is denoted by $\zeta = c_1/c_0 = \tau_3/3\tau_2$, we can write

$$\rho = \max_j |z_j - \zeta + \zeta| \leq |\zeta| + \max_j |z_j - \zeta| = |\zeta| + \rho_0, \tag{4.2}$$

where ρ_0 is the radius of the smallest circle, centered at ζ, circumscribed about P. This suggests that if we employ the *shifted* moments of P,

$$\bar{\tau}_k = k(k-1) \iint_P (z - \zeta)^{k-2} \, dx \, dy, \tag{4.3}$$

these moments will grow only as ρ_0^k instead of ρ^k. (Note that, in practice, these shifted moments are computed from the τ_k by expanding the right-hand side of (4.3) using the binomial theorem. That is, $\bar{\tau}_k$ is a linear combination of $\tau_0, \ldots, \tau_k$.)

If the center of mass ζ is far from the origin, the difference $\rho - \rho_0$ can be quite large, and using shifted moments will therefore certainly improve the condition of H_0. To improve the sensitivity of the problem further, we consider the use of a *scaled* basis for the representation of the moments. A scaled orthogonal family over $D(0,r)$ is derived from the family $\{z^k\}$ as

$$f_k(z) = \frac{z^k}{r^k}. \tag{4.4}$$

In this basis, the scaled and shifted complex moments $\mathbf{t}_k$, which we shall henceforth call *transformed moments*, are given by

$$\mathbf{t}_k = \iint_P f_k''(z - \zeta) \, dx \, dy = \frac{\bar{\tau}_k}{r^k}. \tag{4.5}$$

It is interesting to note the rate of growth of the transformed moments can be significantly tempered by the introduction of the scaling. For simplicity, assume $\zeta = 0$ and invoke (2.7) to get

$$|\mathbf{t}_k| = \frac{|\tau_k|}{r^k} \tag{4.6}$$

$$\leq \frac{1}{r^k} \sum_{j=1}^{n} |a_j| \rho^k \tag{4.7}$$

$$\leq \frac{1}{r^k} n \rho^k. \tag{4.8}$$

Hence, by choosing $r = \rho$, we can ensure that $|\mathbf{t}_k|$ remains bounded! While ρ is not known a priori, it can be estimated from the given moments. Namely, if k is the highest-order moment available, an (under-) estimate of ρ is

$$\widehat{\rho} \approx |\tau_k|^{1/k}, \tag{4.9}$$

which, as we demonstrate in Appendix A, is a consistent estimate of ρ as $k \to \infty$.[2]

Having constructed the transformed moments $\mathbf{t}_k$, we give the corresponding matrix analogous to H_0 in (2.9) by

$$\mathbf{H}_0 = \Phi H_0 \Phi, \tag{4.10}$$

where we give the diagonal matrix Φ by

$$\Phi = \operatorname{diag}\left[\frac{1}{\widehat{\rho}^j}\right]_{j=0}^{n-1}. \tag{4.11}$$

It is important to note that while H_0 is a Hankel matrix, the transformed matrix $\mathbf{H}_0$ is not Hankel in the traditional sense. Rather, it can be classified as having a *generalized* Hankel structure. In any case, $\mathbf{H}_0$ is simply a diagonal scaling of H_0, and given an accurate estimate of ρ, this diagonal scaling will improve the condition number of H_0, as we discuss next.

4.1. Diagonal scaling and improved condition number. Results on improvement of condition number of a matrix by diagonal scaling are scarce [2, 9, 16]. Rather than present a general proof that the diagonal scaling presented above improves the condition number of H_0, we demonstrate this explicitly for a canonical case. Namely, let the vertices z_j be the nth roots of unity: $z_j = \exp(ij\theta)$, where $\theta = 2\pi/n$. The Vandermonde matrix V_n is then simply given by

$$V_n = \sqrt{n} Q_n, \tag{4.12}$$

where Q_n is the (orthogonal) discrete Fourier transform (DFT) matrix of dimension n. Hence, the condition number of V_n is $\kappa_2(V_n) = \kappa_2(Q_n) = 1$. If the vertices z_j are now scaled so that they lie on a circle of radius r, the Vandermonde matrix becomes scaled as

$$V_n(r) = \Delta(r) V_n(1), \tag{4.13}$$

where $\Delta(r) = \operatorname{diag}(1, r, \ldots, r^{n-1})$. The condition number of $V_n(r)$ is then given by

$$\kappa_2\left(V_n(r)\right) = \|\Delta(r) V_n\|_2 \|V_n^{-1} \Delta^{-1}(r)\|_2 \tag{4.14}$$

$$= \sqrt{n} \|\Delta(r)\|_2 \frac{1}{\sqrt{n}} \|\Delta^{-1}(r)\|_2 \tag{4.15}$$

$$= \kappa_2\left(\Delta(r)\right) \tag{4.16}$$

$$= \begin{cases} r^{n-1} & \text{for} \quad r > 1, \\ 1/r^{n-1} & \text{for} \quad r < 1. \end{cases} \tag{4.17}$$

[2] One may estimate ρ using a variety of other techniques. For instance, the ratio τ_{k+1}/τ_k converges to ρ; or we can approximate the characteristic equation. In any event, there appears to be a strong connection to the *epsilon algorithm* [3, 39] here.

Now, to study the structure of the corresponding scaled Hankel matrix $H_0(r) = \Delta(r)H_0(1)\Delta(r)$ we compute the moments τ_k explicitly. Using the expression (2.4) for the coefficients a_j, we have

$$a_j = \sin\theta \exp(-2ij\theta), \tag{4.18}$$

which in turns gives

$$\tau_k = \sum_{j=1}^{n} a_j z_j^k = \sin\theta \sum_{j=1}^{n} e^{ij(k-2)\theta} \tag{4.19}$$

$$= w \sin\theta \sum_{j=0}^{n-1} w^j = w \sin\theta \left(\frac{w^n - 1}{w - 1} \right), \tag{4.20}$$

where $w = \exp(i(k-2)\theta)$ and the last identity holds if $w \neq 1$. However, if $w \neq 1$, then $w^n = \exp(i(k-2)n\theta) = \exp(2\pi i(k-2)) = 1$, and $\tau_k = 0$. Therefore, τ_k is nonzero only when $w = 1$, which occurs for $k = 2,\ n+2,\ 2n+2$, and so on, in which case

$$\tau_2 = \tau_{n+2} = \tau_{2n+2} = \cdots = n \sin\theta. \tag{4.21}$$

This implies that the Hankel matrix H_0 has the following structure:

$$H_0 = H_0(1) = n \sin(\theta)\mathcal{P}(1), \tag{4.22}$$

where $\mathcal{P}(1)$ is a permutation matrix

$$\mathcal{P}(1) = \begin{bmatrix} 0 & 0 & 1 & 0 & \cdots & 0 & 0 \\ 0 & 1 & 0 & 0 & \cdots & 0 & 0 \\ 1 & 0 & 0 & 0 & \cdots & 0 & 0 \\ 0 & 0 & 0 & 0 & \cdots & 0 & 1 \\ 0 & 0 & 0 & 0 & \cdots & 1 & 0 \\ \vdots & \vdots & \vdots & \vdots & \ddots & \vdots & \vdots \\ 0 & 0 & 0 & 1 & \cdots & 0 & 0 \end{bmatrix}. \tag{4.23}$$

As $\mathcal{P}(1)$ is orthogonal, $\kappa_2(H_0(1)) = \kappa_2(\mathcal{P}(1)) = 1$. Meanwhile, the scaled Hankel matrix is

$$H_0(r) = \Delta(r)H_0(1)\Delta(r) = n \sin\theta \Delta(r)\mathcal{P}(1)\Delta(r) = n \sin\theta \mathcal{P}(r). \tag{4.24}$$

The condition number of $\mathcal{P}(r)$ can be found by noting that (assuming $r > 1$)

$$\kappa_2(\mathcal{P}(r)) = \|\mathcal{P}(r)\|_2 \|\mathcal{P}^{-1}(r)\|_2 \tag{4.25}$$

$$= \sqrt{\lambda_{max}\left(\mathcal{P}^T(r)\mathcal{P}(r)\right)} \sqrt{\lambda_{max}\left(\mathcal{P}^T(1/r)\mathcal{P}(1/r)\right)} \tag{4.26}$$

$$= r^{n+2} \frac{1}{r^2} \tag{4.27}$$

$$= r^n. \tag{4.28}$$

Finally, this gives

$$\kappa_2(H_0(r)) = \kappa_2(\mathcal{P}(r)) = r^n, \tag{4.29}$$

which means that scaling the roots of unity to a circle of radius $r > 1$ worsens the condition number of the corresponding Hankel matrix from 1 to r^n. To alleviate this problem, if we know r, we should choose $\Phi = \Delta^{-1}(r) = \Delta(1/r)$. This is the optimum choice of diagonal scaling as it yields

$$\mathbf{H}_0 = \Delta(1/r)H_0(r)\Delta(1/r) = H_0(1), \tag{4.30}$$

which is optimally conditioned. Of course, in reality, we can at best *estimate* r as we described earlier and choose the diagonal scaling according to (4.11). The improvement in condition number will generally not be as good as r^n, since the scaling will not affect the underlying geometry (e.g., eccentricity) of the polygon which is an inherent factor affecting the sensitivity of the inversion problem.

It is worth noting that although the preceding analysis was carried out for $r > 1$, similar scaling issues arise when the vertices are in the interior of the unit circle; that is, when the vertices are significantly smaller than 1 in magnitude.

4.2. Algorithm description. To make the process clear, we present a step-by-step algorithmic description of the shape reconstruction process.

Problem. Given a sequence of moments $\{\tau_k\}_{k=0}^{K-1}$, possibly corrupted by noise, find a polygon to fit these data.

ALGORITHM.

1. Use formula (4.9) to estimate ρ.
2. Shift and scale the moment sequence to obtain the transformed moments $\mathbf{t}_k$.
3. Using the transformed moments, estimate the number n of vertices using singular value or minimum description length (MDL) techniques. (See section 5.)
4. Form the *generalized* Hankel matrices $\mathbf{H}_0$ and $\mathbf{H}_1$ using the transformed moments. If the number of moments $K > 2n$, $\mathbf{H}_0$ and $\mathbf{H}_1$ can be formed as rectangular matrices with $K - n$ rows and n columns.
5. Solve the generalized eigenvalue problem

$$\mathbf{H}_1\mathbf{u} \;=\; z\,\mathbf{H}_0\mathbf{u} \tag{4.31}$$

   using the QZ algorithm, starting with the QR algorithm as described in section 3. If $\mathbf{H}_0$ and $\mathbf{H}_1$ are rectangular, the generalized eigenvalues of the corresponding normal equations are needed, and again one can use the QR factorization described earlier to begin the QZ process and thus avoid forming the normal equations.[3] The true vertices are then given by the computed eigenvalues shifted according to the estimate of the center of mass $\tau_3/3\tau_2$.
6. Solve for the parameters a_j using Vandermonde or least-squares methods.
7. Solve for the angles ϕ_j and (if possible) solve for the interior of the polygon.

5. Optimal number of vertices. Given a sequence of moments τ_k, or the transformed moments $\mathbf{t}_k$, the structure of the Hankel matrix H_0 shown earlier assumes knowledge of the number of vertices n. In practice, this is not the case. In particular, if the given moment sequence is not corrupted by noise, we may form the largest H_0 possible. The rank of this matrix will then be equal to the number of underlying

[3]Forming the normal equation, while useful in canceling out the effects of noise, can result in a (more) ill-conditioned square system. Another possibility is using Kung's method [24] whereby the truncated SVD of $\mathbf{H}_1$ and $\mathbf{H}_0$ are used to form and solve a square pencil.

vertices n. If the given moment sequence is corrupted by noise, however, the rank estimation problem is more difficult as H_0 will, almost always, have full rank as a result of the noise. Several approaches have been suggested [34, 37]. The common theme among these is that by observing the behavior of the (descending ordered) sequence of singular values of H_0, one may observe a sharp "break" in the rate of decrease of these values. This break point then can be identified as the boundary between the signal and noise components. That is, the singular values before the break will correspond to the true signal, and hence the number of such singular values will correspond to the number of signal components (or vertices) which we seek. Naturally, the difficulty with this approach is that this *break point* is hardly ever easy to identify as no rigorous analysis for this choice has been carried out.

Another approach is the use of the MDL principle of Rissanen [30]. The interpretation of vertex reconstruction as an array processing problem allows for the use of the MDL principle derived for array processing applications by Wax and Kailath in [38]. In this framework, data containing the superposition of a finite number of signals, corrupted by additive noise, is measured at a collection of m spatially separated sensors, yielding data vectors $d(t_i) = [d_1(t_i), d_2(t_i), \ldots, d_M(t_i)]^T$. Each vector $d(t_i)$ is a *snapshot* at a fixed time t_i across the array of sensors. Next, the signal covariance matrix is estimated from the data as follows:

$$\widehat{R} = \frac{1}{N}\sum_{i=1}^{N} d(t_i)d^H(t_i). \tag{5.1}$$

If the eigenvalues $\lambda_1, \lambda_2, \ldots, \lambda_M$ of $\widehat{R}$ are arranged in descending order, the MDL cost function defined over integer values n is

$$MDL(n) = -\log\left[\frac{\prod_{i=n+1}^{M}\lambda_i^{\frac{1}{M-n}}}{\frac{1}{M-n}\sum_{i=n+1}^{M}\lambda_i}\right]^{(M-n)N} + \frac{n}{2}(2M-n)\log(N), \tag{5.2}$$

which, when minimized, has been shown [38] to produce a consistent estimate $\widehat{n}$ of the number of signals. It is interesting to note that the bracketed part of the first term in the above expression is simply the ratio of the geometric mean to the arithmetic mean of the smallest $M-n$ eigenvalues of $\widehat{R}$.

In our application, the given data are the elements of the moment sequence $\{\tau_k\}_{k=0}^{K-1}$ or $\{\mathbf{t}_k\}_{k=0}^{K-1}$ and there is no time dependence per se. What we have, in effect, is a single snapshot of data across a possibly large array, each index k representing one sensor in that array. A process called *spatial smoothing* can be applied to map our scenario to the standard framework. More specifically, as in [1] we can divide the given moment sequence into N subvectors ν_i, each of length M, where M is such that $\bar{n} < M \leq K - \bar{n} + 1$, with $\bar{n}$ being the largest expected number of vertices. This will ensure that the estimated covariance matrix

$$\widehat{R} = \frac{1}{N}\sum_{i=1}^{N}\nu_i\nu_i^H \tag{5.3}$$

will have rank at least $\bar{n}$. While choosing M large will help to dampen out the effect of the noise, it also means that the size of $\widehat{R}$ will be large and therefore increases the computational load of the algorithm. In addition, a large M will imply a small N, and this, in turn, affects how well the estimated covariance matrix approximates the

true covariance matrix. To get the largest possible N for a choice of M, we therefore need the vectors ν_i to be maximally overlapping; hence we set $N = K+1-M$. It has been suggested that the choice $M = \sqrt{K}$ tends to give satisfactory results. Another reference [13] suggests that for shorter data records (K) and/or closely spaced sources (vertices), the choice $M \approx 0.6(K+1)$ is best. We have observed that using the transformed moments $\mathbf{t}_k$ we can obtain estimates of the number of sides that, while not often exact, are reasonably close to the true values.

6. An application to geophysical inversion. The above results can be useful in several areas of application. Among these, we outlined the application to tomography in [27] where the measured data are (tomographic) projections of the polygon and from which the moments can be uniquely estimated. In what follows, we describe a different application area, namely, the problem of geophysical inversion from gravimetric measurements [29, 35].

A somewhat unexpected application of the results obtained in this paper and in [27] is found in the field of gravimetric and magnetometric geophysical inversion. For the gravimetric application, it is of interest to reconstruct the shape and (possibly) density of a gravitational anomaly from discrete measurements of the exterior gravitational field at spatially separated points. In particular, consider the problem of reconstructing the boundary of an arbitrary simply connected region P, and the mass density $f(x,y)$ within it, from measurements of its gravitational field $G(x,y)$ made at points in the plane outside of P. In practice, it is often convenient to assume that P is a *cross-sectional slice* of a 3D body $\mathbf{P}$ of infinite extent (l) and density $f(x,y,l) = f(x,y,0) = f(x,y)$. That is, for each l, $\mathbf{P}$ is simply a replica of P in terms of both shape and density. Under this assumption, the *exterior* potential $\phi(x,y)$ due to the object is a harmonic function[4] which behaves as $c\log(x^2+y^2)^{1/2}$ for some constant c [35]. This class of potential functions is referred to as *logarithmic* potentials that are limiting cases of the standard Newtonian potentials for (cylindrical) objects of infinite extent [22].

The (vector) field $G(x,y) = \nabla\phi$ can be embedded in the complex plane by defining the variable $\xi = x + iy$ and writing

$$G(\xi) = \frac{\partial\phi}{\partial x} \; + \; i\,\frac{\partial\phi}{\partial y}, \tag{6.1}$$

where $G(\xi)$ is now, by construction, an analytic function outside of P. Under mild constraints this analytic function admits an integral representation:

$$G(\xi) = 2ig\iint_P \frac{f(x',y')}{\xi-\xi'}\,dx'\,dy', \tag{6.2}$$

where $\xi' = x' + iy'$, and where g is the universal gravitational constant. For values of ξ outside of P, we can expand the field into an asymptotic series as follows:

$$G(\xi) = 2ig\iint \frac{1}{\xi}\,\frac{1}{1-(\xi'/\xi)} f(x',y')\,dx'\,dy' \tag{6.3}$$

$$= 2ig\iint \frac{1}{\xi}\sum_{k=0}^{\infty}\left(\frac{\xi'}{\xi}\right)^k f(x',y')\,dx'\,dy' \tag{6.4}$$

$$= 2ig\sum_{k=0}^{\infty} c_k\,\xi^{-(k+1)}, \tag{6.5}$$

[4] One that satisfies Laplace's equations: $\nabla^2\phi = 0$.

where the coefficients c_k are the moments

$$c_k = \iint_P f(x,y)\, z^k \, dx\, dy, \tag{6.6}$$

which for a uniform density $f(x,y) = 1$ are called the harmonic moments and were defined in (2.5). Therefore, we observe that if the field $G(\xi)$ is known, then the moments c_k are determined and hence the inverse potential problem is equivalent to the reconstruction of $f(x,y)$ and the region P from its moments.

In particular, let us consider a truncated asymptotic expansion of G,

$$G(\xi) = 2ig \sum_{k=0}^{K-1} c_k\, \xi^{-(k+1)}, \tag{6.7}$$

and assume that at least K measurements $G(\xi_1), G(\xi_2), \ldots, G(\xi_K)$ are given (at points away from $\xi = 0$). Collecting these in vector form and rewriting, we have the Vandermonde system

$$\begin{bmatrix} \xi_1 G(\xi_1) \\ \xi_2 G(\xi_2) \\ \vdots \\ \xi_K G(\xi_K) \end{bmatrix} = 2ig \begin{bmatrix} 1 & \xi_1^{-1} & \cdots & \xi_1^{-(K-1)} \\ 1 & \xi_2^{-1} & \cdots & \xi_2^{-(K-1)} \\ \vdots & \vdots & & \vdots \\ 1 & \xi_K^{-1} & \cdots & \xi_K^{-(K-1)} \end{bmatrix} \begin{bmatrix} c_0 \\ c_1 \\ \vdots \\ c_{K-1} \end{bmatrix} = \Xi_K\, C_K. \tag{6.8}$$

This Vandermonde system is not unlike the ones we encountered in the earlier sections. The Vandermonde matrix (Ξ_K) on the right-hand side is invertible if and only if the measurements are made at spatially separated points, but this inversion is not always stable. In particular, the condition of the above Vandermonde system is dependent upon the location of the ξ_k. The results of [12] and section 4.1 imply that for best conditioning these points should be placed at the roots of unity, if this is indeed practicable. If not, scaling results similar to those of section 4.1 can be derived and applied to this problem as well for improved conditioning.

For the case where $f(x,y)$ is a uniform density and P is a simply connected polygonal region, once we have solved (6.8) for the moments c_k, we can proceed as before with the approximate reconstruction of P as a polygon. In contrast to the tomographic application discussed in [27], the reconstruction algorithm described above for the gravimetric problem is, strictly speaking, approximate even if the measurements of the field are exact, and the underlying P is, in fact, polygonal. This is because the algorithm is dependent upon the *truncated* series in (6.7). It is worth noting, however, that the series (6.7) converges to the true value of G quite quickly.

Finally, we mention that the results described above are also important and applicable to a variety of inverse problems such as thermal conductivity and others arising from general elliptic integral equations [35].

7. Numerical examples. In this section we present three numerical examples to illustrate the main points of the paper. In particular, the first two examples illustrate the sensitivity of the computations involved, while the third example demonstrates the application to the geophysical gravimetric inverse problem discussed in section 6 and also how the MDL procedure described in section 5 can be used to estimate the number of vertices.

7.1. Example 1. This example illustrates the sensitivity associated with vertices which are closely spaced or which have small interior angles. The polygon (shown in Figure 1) is a triangle with a small triangular slit (of width 2α) cut out of one side. We have chosen $\alpha = 10^{-3}$ for this example. The results (using MATLAB and IEEE floating-point standard arithmetic) are shown in Table 7.1. The moments are generated from the actual vertices z_j, and from these simulated "measurements" the estimated vertices $\widehat{z}_j$ and coefficients $\widehat{a}_j$ are computed. To emphasize the sensitivity of the problem, we assume that the value of ρ is known exactly. Then the vertices are estimated by using the QZ algorithm [15] on the generalized eigenvalue problem estimated from the *transformed* moments. For reference, we note that the condition number of the Hankel matrix H_0 is $\kappa_2(H_0) = 3.6 \times 10^8$, whereas the condition of the Hankel matrix corresponding to the transformed moments is $\kappa_2(\mathbf{H}_0) = 2.9 \times 10^4$—a significant improvement.

The coefficients $\widehat{a}_j$ are computed by inverting the Vandermonde system (3.13). Therefore, not surprisingly, the errors in $\widehat{a}_j$ can be larger than for the corresponding vertices, by a factor equal to the condition number of V, which is $\kappa_2(V) = 5.7 \times 10^3$. Also shown are the sensitivity factors s, which are simply the right-hand side of (3.23); note that they predict the accuracy of the estimated vertices quite well.

TABLE 7.1
Table of errors and sensitivities for Example 1.

z	$\lvert z - \widehat{z}\rvert$	$\lvert a - \widehat{a}\rvert$	s
1.0	2.0×10^{-12}	2.0×10^{-14}	5.0×10^4
$2 + 0.001i$	1.1×10^{-9}	1.5×10^{-6}	1.5×10^7
$2 + i$	10^{-15}	10^{-15}	13
0.0	10^{-15}	10^{-15}	3.6
$2 - i$	10^{-15}	10^{-14}	13
$2 - 0.001i$	1.1×10^{-9}	1.5×10^{-6}	1.5×10^7

7.2. Example 2. This example (see Figure 2) demonstrates that the computations can be sensitive even when the underlying polygon contains no small (or large) angles. Here the polygon is the block "E," with all angles equal to 90°. The Vandermonde matrix V has condition number 9×10^{10} and the Hankel matrix H_0 has condition number 4×10^{13}, whereas the Hankel matrix of transformed moments $\mathbf{H_0}$ has condition number 1.4×10^7. The results are given in Table 7.2. Again, the accuracy is predicted well by the sensitivity factors s.

7.3. Example 3. In this example, we demonstrate the application of the algorithm to the problem of shape reconstruction from gravitational field measurements. Specifically, we produce simulated measurements of the gravitational field due to the solid object shown in Figure 3. For convenience we choose to simulate these measurements at equally spaced points (roots of unity) on the unit circle as again shown in Figure 3. While this is admittedly rather unrealistic, it helps us to more clearly carry out the example, since with this choice the Vandermonde system in (6.8) is optimally conditioned.

A total of 20 measurements of the gravitational field were simulated in the clockwise direction at roots of unity starting at $\xi = 1$ (using the exact formula for the field due to a planar polygon, which is described in [35]). The magnitude and phase of the simulated measurements $G(\xi)$ are shown in Figure 4. These values were then corrupted by (complex) Gaussian white noise with standard deviation $\sigma = 2 \times 10^{-3}$.

TABLE 7.2
Table of errors and sensitivities for Example 2.

z	$\lvert z-\widehat{z}\rvert$	$\lvert a-\widehat{a}\rvert$	s
$1+i$	6.4×10^{-10}	1.2×10^{-8}	1.5×10^{7}
$0.5+i$	9.3×10^{-10}	1.3×10^{-8}	2.0×10^{7}
$0.5+2i$	2.0×10^{-10}	3.7×10^{-9}	6.6×10^{6}
$1+2i$	1.3×10^{-10}	2.9×10^{-9}	4.2×10^{6}
$1+3i$	1.7×10^{-13}	5.3×10^{-12}	7.3×10^{3}
$3i$	8×10^{-14}	1.7×10^{-12}	3.8×10^{3}
$-3i$	9×10^{-14}	1.9×10^{-12}	3.8×10^{3}
$1-3i$	1.7×10^{-13}	4.9×10^{-12}	7.3×10^{3}
$1-2i$	1.3×10^{-10}	3.0×10^{-9}	4.2×10^{6}
$0.5-2i$	2.1×10^{-10}	3.8×10^{-9}	6.6×10^{6}
$0.5-i$	9.4×10^{-10}	1.4×10^{-8}	2.0×10^{7}
$1-i$	6.5×10^{-10}	1.2×10^{-8}	1.5×10^{7}

From these noisy data, the first 20 complex moments c_k of the underlying shape were computed, allowing reconstructions with up to 10 vertices. From these computed moments, the transformed moments $\mathbf{t}_k$ were computed. The MDL values and the singular values of the matrix $\mathbf{H}_0$ are displayed in Figure 5. Note that the MDL criterion indicates the correct number of vertices (namely, 4), whereas the singular value approach underestimates the number of vertices to 3. The reconstruction using four vertices is shown as the dashed polygon in Figure 3. As is apparent, this is a rather nice approximation to the underlying shape.

8. Summary and extensions. In this paper we presented a stable numerical solution for the problem of shape reconstruction from moments. This problem has many applications including tomographic reconstruction [27] and geophysical inver-

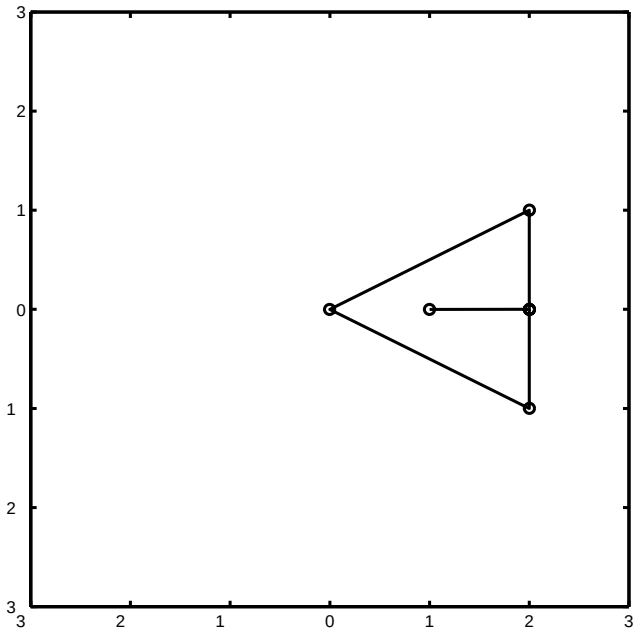

FIG. 1. *The six-sided polygon of Example* 1.

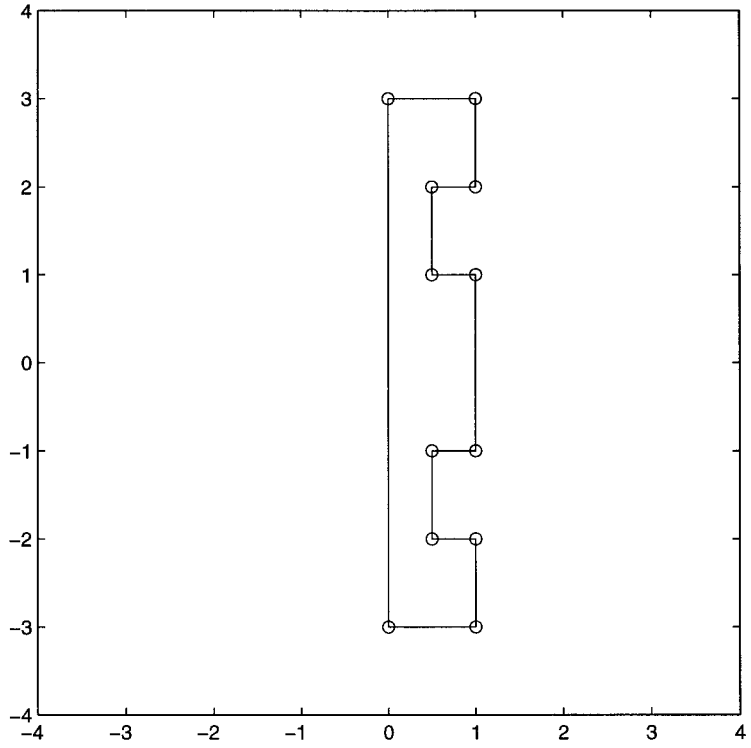

FIG. 2. *The twelve-sided polygon of Example* 2.

sion. A rather remarkable feature of this moment problem is that it can be thought of as the dual of the problem of numerical quadrature in two dimensions. Some important and interesting questions remain to be addressed regarding this problem:

- The study of statistical procedures for obtaining optimal estimates of the vertices based upon the techniques presented here is important. In practically all applications, the effect of noise is significant and must be dealt with. The literature on array signal processing [23] has dealt with this question in depth. However, the statistical algorithms developed in that area are built around specific signal models which do not hold in the context of shape reconstruction (specifically, the assumption that the sources—our vertices—lie on the unit circle). Therefore, many of the scaling issues we have dealt with in this paper never arise in the existing array processing literature.
- Regularization of the shape reconstruction problem by inclusion of prior geometric models may significantly improve the robustness of these techniques. For instance, constraints such as convexity and the inclusion of terms which penalize excessive (discrete) curvature in the resulting solutions can yield useful and computationally interesting extensions of the algorithms presented here.

It is our hope that the results of this paper along with the above observations will stimulate further work in this area both in terms of new numerical and statistical techniques and also in terms of applications of these techniques to solving physical

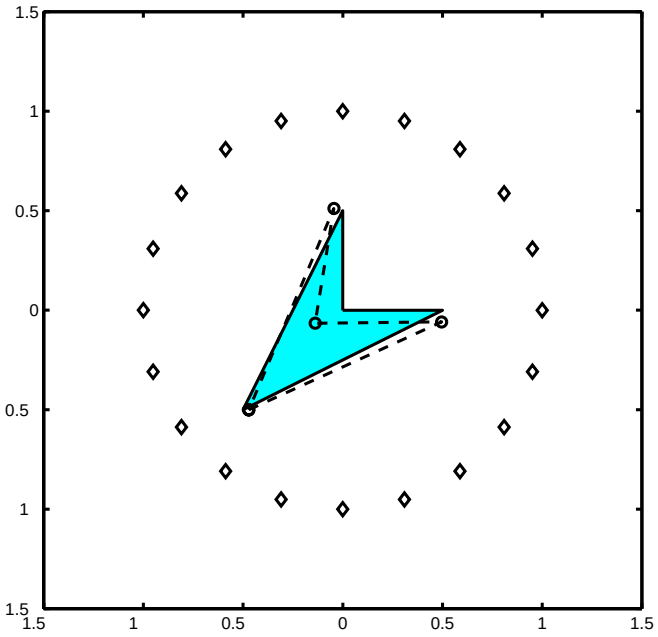

FIG. 3. *The underlying polygon (-), the reconstructed polygon (- -), and the locations of the gravity probes (diamonds) for Example* 3.

problems.

Appendix A. Proof of convergence of ρ estimate.

LEMMA A.1. *Consider the sequence* $q_k = |\tau_k|^{1/k}$. *Then* $q_k \to \rho$, *except possibly for a subsequence* $q_{k_j} \to 0$.

Proof. Since

$$\tau_k = \sum_{j=1}^{k} a_j z_j^k, \tag{A.1}$$

the behavior of the $\{\tau_k\}$ is essentially that of the power method (see Golub and Van Loan [15]). If $\rho = |z_1| > |z_j|,\ j = 2, \ldots, n$, then

$$\tau_k = a_1 z_1^k \left(1 + \sum_{j>1} \frac{a_j}{a_1} \left(\frac{z_j}{z_1} \right)^k \right), \tag{A.2}$$

and $|z_j/z_1| \le \sigma < 1$. (Recall also that $a_j \neq 0$.) Thus $|\tau_k|^{1/k} \to |z_1| = \rho$, with the rate of convergence depending on σ.

When two or more vertices have the same modulus ρ, the behavior is more complicated. The general case can be illustrated as follows: suppose $\rho = |z_1| = |z_2| > |z_j|,\ j = 3, \ldots, n$. Then

$$\tau_k = a_1 z_1^k \left(1 + \frac{a_2}{a_1} e^{ik\theta_1} + \sum_{j>2} \frac{a_j}{a_1} \left(\frac{z_j}{z_1} \right)^k \right), \tag{A.3}$$

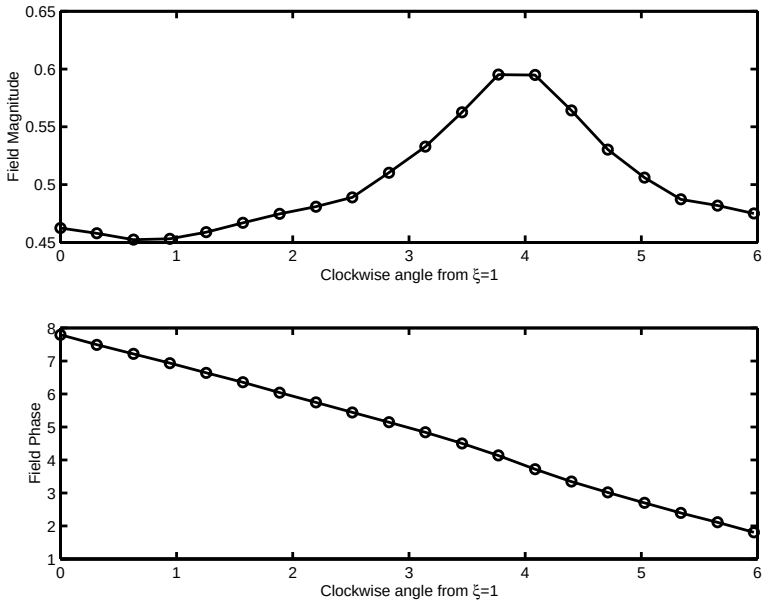

FIG. 4. *The magnitude and phase of the complex gravity field measurements for Example* 3.

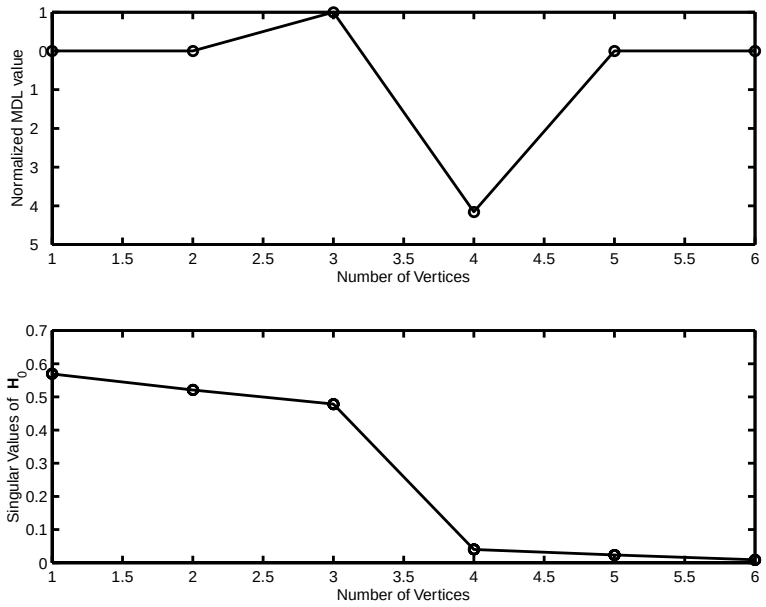

FIG. 5. *MDL and SVD values for determining the number of vertices in Example* 3.

where $z_2/z_1 = e^{i\theta_1}$. The points $w_k = 1 + \frac{a_2}{a_1} e^{ik\theta_1}$ all lie on the curve $w(\theta) = 1 + \frac{a_2}{a_1} e^{i\theta}$, and they all satisfy $|w_k|^{1/k} \to 1$ except for those points $w_{k_j} = 0$, if in fact the curve $w(\theta)$ goes through the origin. This can only happen if $1 + \frac{a_2}{a_1} e^{ik\theta_1} = 0$, which implies $\frac{a_2}{a_1} = e^{ik\theta_2}$, with $k\theta_1 + \theta_2 = \pi \pm 2j\pi$. The set of values $\{k_j\}$ for which this occurs may be finite or a subsequence (for instance, if $z_1 = 1,\ z_2 = -1,\ a_1 = a_2 = 1$, it occurs for

all odd integers). Clearly, apart from this subsequence $\{k_j\}$, $|\tau_k|^{1/k} \to \rho$. □

REFERENCES

[1] H. K. Aghajan and T. Kailath, *SLIDE: Subspace-based line detection*, IEEE Transactions on Pattern Analysis and Machine Intelligence, 16 (1994), pp. 1057–1073.

[2] F. Bauer, *Optimally scaled matrices*, Numer. Math., 5 (1963), pp. 73–87.

[3] C. Brezinski and M. Redivo-Zaglia, *Extrapolation Methods: Theory and Practice*, North–Holland, Amsterdam, 1991.

[4] M. Brodsky and E. Panakhov, *Concerning a priori estimates of the solution of the inverse logarithmic potential problem*, Inverse Problems, 6 (1990), pp. 321–330.

[5] P. Davis, *Interpolation and Approximation*, Dover, New York, 1963.

[6] P. Davis, *Triangle formulas in the complex plane*, Math. Comp., 18 (1964), pp. 569–577.

[7] P. Davis, *Plane regions determined by complex moments*, J. Approx. Theory, 19 (1977), pp. 148–153.

[8] P. Diaconis, *Application of the method of moments in probability and statistics*, in Proc. Sympos. Appl. Math., AMS, Providence, RI, 37 (1987), pp. 125–142.

[9] G. Forsythe and E. Straus, *On best conditioned matrices*, Proc. Amer. Math. Soc., 6 (1955), pp. 340–345.

[10] V. Fraysse and V. Toumazou, *A note on the norm-wise perturbation theory for the regular generalized eigenvalue problem*, Numer. Linear Algebra Appl., 5 (1998), pp. 1–10.

[11] W. Gautschi, *On the construction of Gaussian quadrature rules from modified moments*, Math. Comp., 24 (1970), pp. 245–260.

[12] W. Gautschi and G. Inglese, *Lower bounds for the condition number of Vandermonde matrices*, Numer. Math., 52 (1988), pp. 241–250.

[13] A. B. Gershman and V. T. Ermolaev, *Optimal subarray size for spatial smoothing*, IEEE Signal Processing Letters, 2 (1995), pp. 28–30.

[14] G. Golub and M. Gutknecht, *Modified moments for indefinite weight functions*, Numer. Math., 57 (1990), pp. 607–624.

[15] G. Golub and C. Van Loan, *Matrix Computations*, Johns Hopkins University Press, Baltimore, MD, 1996.

[16] G. Golub and J. Varah, *On a characterization of the best l_2-scaling of a matrix*, SIAM J. Numer. Anal. 11 (1974), pp. 472–479.

[17] D. Higham and N. Higham, *Structured Backward Error and Condition of Generalized Eigenvalue Problems*, Department of Mathematics, University of Manchester, Tech. report; SIAM J. Matrix Anal. Appl., submitted.

[18] N. Higham, *Accuracy and Stability of Numerical Algorithms*, SIAM, Philadelphia, 1996.

[19] A. Hildebrand, *Introduction to Numerical Analysis*, McGraw–Hill, New York, 1956.

[20] J. Howland, *On the Construction of Gaussian Quadrature Formulae*, manuscript, 1975.

[21] Y. Hua and T. Sarkar, *Matrix pencil method for estimating parameters of exponentially damped/undamped sinusoids in noise*, IEEE Transactions on ASSP, 38 (1990), pp. 814–824.

[22] O. Kellog, *Foundations of Potential Theory*, Dover, New York, 1953.

[23] H. Krim and M. Viberg, *Two decades of array signal processing*, IEEE Signal Proceedings Mag., 13 (1996), pp. 67–94.

[24] S. Y. Kung, K. S. Arun, and B. D. Rao, *State-space and singular value decomposition-based approximation methods for the harmonic retrieval problem*, J. Opt. Soc. Amer., 73 (1983), pp. 1799–1811.

[25] F. Luk and D. Vandevoorde, *Decomposing a signal into a sum of exponentials*, in Iterative Methods in Scientific Computing, R. Chan, T. Chan, and G. Golub, eds., Springer-Verlag, Singapore, 1997, pp. 329–357.

[26] P. Milanfar, W. Karl, and A. Willsky, *A moment-based variational approach to tomographic reconstruction*, IEEE Trans. Image Proc., 5 (1996), pp. 459–470.

[27] P. Milanfar, G. Verghese, W. Karl, and A. Willsky, *Reconstructing polygons from moments with connections to array processing*, IEEE Trans. Signal Proc., 43 (1995), pp. 432–443.

[28] C. Moler and G. Stewart, *An algorithm for generalized matrix eigenvalue problems*, SIAM J. Numer. Anal., 10 (1973), pp. 241–256.

[29] R. Parker, *Geophysical Inverse Theory*, Princeton University Press, Princeton, NJ, 1994.

[30] J. Rissanen, *Modeling by shortest data description*, Automatica, 14 (1978), pp. 465–471.

[31] R. Roy, A. Paulraj, and T. Kailath, *ESPRIT: A subspace rotation approach to estimation*

of parameters of cissoids in noise, IEEE Trans. ASSP, ASSP-34 (1986), pp. 1340–1342.

[32] I. Schoenberg, *Approximation: Theory and Practice*, Stanford University, 1955. Notes on a series of lectures at Stanford University.

[33] M. I. Sezan and H. Stark, *Incorporation of a priori moment information into signal recovery and synthesis problems*, J. Math. Anal. Appl., 122 (1987), pp. 172–186.

[34] G. Stewart, *Determining the rank in the presence of error*, in Linear Algebra for Large-Scale and Real-Time Applications, Moonen, Golub, and DeMoor, eds., Kluwer Academic Publishers, Norwell, MA, 1992.

[35] V. Strakhov and M. Brodsky, *On the uniqueness of the inverse logarithmic potential problem*, SIAM J. Appl. Math., 46 (1986), pp. 324–344.

[36] E. Tyrtyshnikov, *How bad are Hankel matrices?*, Numer. Math., 67 (1994), pp. 261–269.

[37] D. Vandevoorde, *A Fast Exponential Decomposition Algorithm and Its Application to Structured Matrices*, Ph.D. thesis, Dept. of Computer Science, Rensselaer Polytechnic Institute, October 1996.

[38] M. Wax and T. Kailath, *Detection of signals by information theoretic criteria*, IEEE Trans. ASSP, ASSP-33 (1985), pp. 387–392.

[39] P. Wynn, *On a device for computing the $e_m(S_n)$ transformation*, MTAC, 10 (1956), pp. 91–96.